AD

EARTHQUAKE ENGINEERING SUPPORT PHASE 4

Final Technical Report

by

R S Steedman

September 2000

United States Army

EUROPEAN OFFICE OF THE U.S. ARMY

London England

CONTRACT NUMBER: N68171-00-M-5505

PRINCIPAL INVESTIGATOR: DR R S STEEDMAN

SUMMARY

This report describes the initial findings of an experimental study supported by the U.S. Army Centrifuge Research Center and Engineer Earthquake Engineering Research Program (EQEN) into the behavior of saturated sands under high initial effective confining stresses subjected to strong ground shaking. The research was conducted using the Army Centrifuge at the U.S. Army Engineering Research and Development Center (ERDC), located in Vicksburg MS, formerly known as the Waterways Experiment Station (WES). The centrifuge studies have shown that the generation of excess pore pressure is limited to a level less than 100 percent for vertical effective confining stresses exceeding around 3 atmospheres (atm, or 300 KPa). This limit reduces at higher confining stresses. It is likely that this limit is a function of a range of variables, including amplitude of shaking. A second key finding indicates that dense layers overlying loose layers may still be readily liquefied as a consequence of the high excess pore pressures generated below. If verified, the potential benefits from these findings for the design of remediation works for large earth dams could be substantial. The report describes the equipment used for the experiments, the research program, and presents the initial results, contrasting the development of excess pore pressure at low confining stress with that at high confining stress. Possible consequences for a hypothetical dam are discussed.

LIST OF KEYWORDS

liquefaction
centrifuge
earthquake
model
experiment
sand
dam safety

TABLE OF CONTENTS

1.0 BACKGROUND

This research contract addressed the fourth phase in the completion of an experimental and analytical research programme in support of the Earthquake Engineering Research Program under the direction of the USAE ERDC (formerly the Waterways Experiment Station), Vicksburg, Mississippi. This study was a continuation of earlier research under Contract Nos. N68171-98-C-9014, N68171-97-M-5710, N68171-97-C-9012 and N68171-99-C-9021. The research involved further interpretation of the experimental data, preparation of technical papers for publication and the commissioning of the new MkII large earthquake actuator, based on a substantial remodeling and upgrading of the MkI unit. The work was completed in September 2000.

2.0 INTRODUCTION

The current state-of-practice for the evaluation of liquefaction potential and for remediation design and analysis depends on empirical correlations of in-situ measurements of strength versus field experience of liquefaction at shallow depth and laboratory data of the behavior of confined elements under cyclic loading. (Liquefaction is defined here to mean the development of pore pressure equal to 100% of the initial vertical effective stress.) This approach is known as the "simplified procedure". Opinions vary as to the maximum depth in the field at which liquefaction has been observed, but there is no established field evidence from historic earthquakes of liquefaction at depths greater than a few tens of meters. The NCEER Workshop in 1996 on the Evaluation of Liquefaction Resistance of Soils noted that the simplified procedure was developed from evaluations of field observations and field and laboratory test data, Youd and Idriss (1997). The report notes, "These data were collected mostly from sites ... at shallow depths (less than 15m). The original procedure was verified for and is applicable only to these site conditions".

Hence, in design practice the assessment of liquefaction under high initial effective confining stress, such as might relate to the foundations of large earth dams, is based on the extrapolation of observed behavior and correlations at shallow depths. In practice, the behavior of saturated soil under these conditions is not well understood. Based on the results of laboratory tests, researchers have postulated that there is a reduction in the liquefaction resistance of such soil compared to shallow depths. This reduction is accounted for in standard approaches by a ratio known as K_σ, a "correction factor" developed by Seed (1983) in the simplified procedure. This strength ratio is postulated to reduce with increasing initial effective confining stress, which has a large impact potentially on the extent and method (hence cost) of remedial construction required to assure adequate seismic performance of large dams. For example, it may reduce the cyclic shear stress ratio predicted to cause liquefaction in a soil layer under a typical large dam (of the order of 30m high) to about 50% of its value in the absence of the dam. The predicted deformations and resistance and the remedial strength required are a direct function of the reduced shear strength. The K_σ strength reduction therefore

has a strong influence on the decision to remediate a large dam and on the costs of that remediation.

The factor K_σ quantifies the curvature in the cyclic shear strength envelope (cyclic shear stress required to cause liquefaction versus confining stress) for a soil as observed in laboratory tests on discrete specimens. Although some curvature may be expected, such large reductions in cyclic shear strength ratios are counter-intuitive. It is generally accepted that increased confining stress should broadly improve the capacity of a soil to resist applied loads, not reduce it. Clearly the volume of soil that requires to be treated and the difficulty and expense of that treatment are highly dependent on an accurate assessment of the potential for and consequences of liquefaction.

There is therefore strong motivation for owners of large dams to investigate the behavior of saturated sands subject to strong ground shaking under high initial effective confining stresses. In the absence of field data, the use of a centrifuge was considered to be the only practical option to realistically represent a deep soil deposit subjected to earthquake shaking. The studies reported in this report relate exclusively to level ground initial stress conditions in a two-layer (dense over loose) deposit of clean, fine Nevada sand. Examination of more complex stratigraphy and sloping ground stress conditions is planned for future studies.

3.0 THE ERDC CENTRIFUGE, EARTHQUAKE ACTUATOR AND ESB SPECIMEN CONTAINER

The design specification for the ERDC centrifuge followed a review of the Army's research needs and a study of the available academic facilities, Ledbetter (1991). Many of the field problems with which the U.S. Army Corps of Engineers is concerned are physically large, such as earth dams, locks and river control structures, environmental problems and military research. It was determined that a new facility with a high payload capacity and high g capability was required to meet future Army needs. A large beam centrifuge was commissioned, termed the Acutronic 684, based on the French designed Acutronic 661, 665 and 680 series of geotechnical centrifuges, Ledbetter et al. (1994a). The capacity of the ERDC centrifuge is a payload of 8 tonnes at up to 143 g, reducing to 2 tonnes at 350 g, with a platform area of 1.3m square. This high capacity enables field problems of the order of up to 300m in breadth, 300m in depth, and 1000m in length to be simulated under a wide variety of loading conditions. The facility is now fully operational, and is equipped with a large range of equipment and appurtenances, Figure 1.

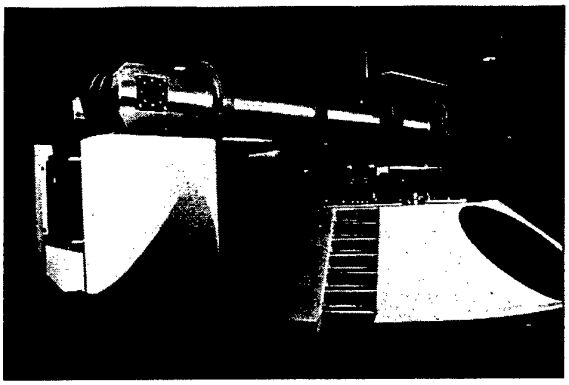

Figure 1. The WES centrifuge

The research approach for this high confining stress liquefaction study uses the large capacity of the WES centrifuge to investigate the generation of excess pore pressure and liquefaction under conditions that much more closely resemble those at depth in the field, Ledbetter et al. (1999). To do this required the design and construction of a large dynamic actuator.

3.1 Shaker design

A mechanical design was adopted for the earthquake actuator for the ERDC centrifuge, based closely on a smaller version designed for Cambridge University, England. Complex servo-hydraulic shaking systems have been developed and are operational on several centrifuges around the world, but these are limited in the g level to which they may operate, and are considerably more expensive to build. The research by ERDC into the basic behavior of liquefying soils and comparison with present design methods required a base motion comprising a series of uniform cycles of base shaking, of variable duration and uniform frequency. A rotating mechanical system is ideally suited for this purpose. The large carrying capacity of the centrifuge meant that the shaker itself could act as the reaction mass for the specimen, minimizing the vibrations that would be otherwise transmitted to the centrifuge itself, and the model container could be much deeper and longer than usual.

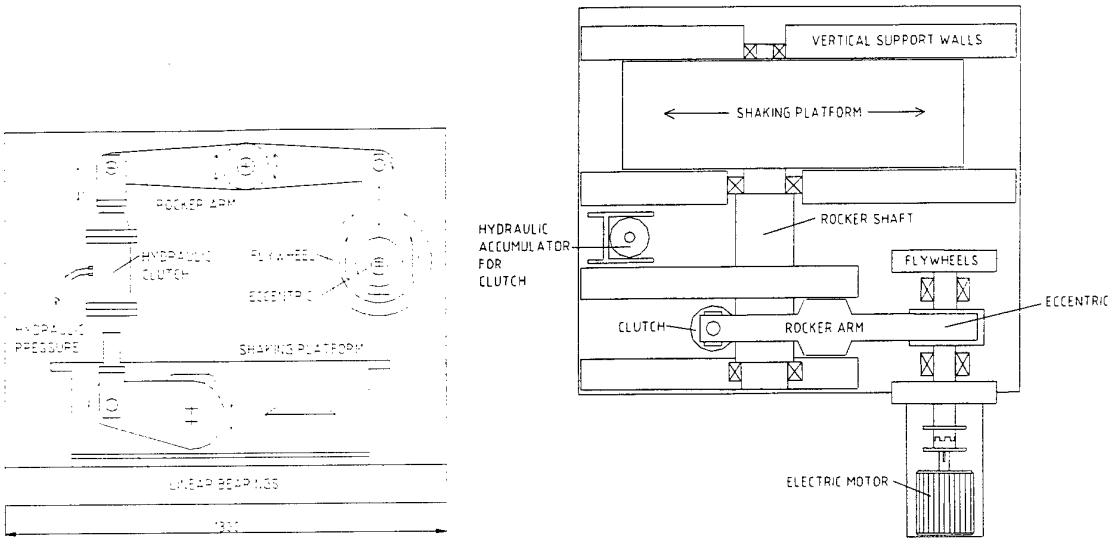

Figure 2. The ERDC Mk I earthquake actuator

The principle of the operation of the Mk I shaker was based on the use of stored energy to drive the specimen back and forth. Flywheels are incorporated in the shaker mechanism to store the energy in advance of the shaking event in the form of stored angular momentum. A system of linkages and eccentrics transferred the stored energy of the fly wheels to the shaking platform and thence into the soil specimen, Figure 2. A hydraulic or electrical motor drove the flywheels up to full speed, and then, on a signal, a high speed clutch grabbed the oscillating shaft and transferred energy into the model until another signal released it again. Clearly the frequency of the oscillation was directly proportional to the speed of the motor (and flywheels). The amplitude was controlled by the arrangement of the eccentrics; three displacement amplitudes for the platform were available (+/- 0.49mm, +/-1.47mm and +/-4.41mm).

The shaker was designed (structurally) for operation up to 150g, at which the maximum load capacity of the shaking platform is reached (75 tonnes). The design maximum lateral force, which the mechanism could exert on the shaking platform, was 30 tonnes and the maximum frequency at which the shaker could be safely operated was 150 Hz (eg. 1Hz prototype at 150g, or 3Hz prototype at 50g). (The Mk I shaker was upgraded during 2000 to enable larger amplitude shaking.)

3.2 Model containment

The specimen is built within a hollow rectangular model container, termed an equivalent shear beam (ESB) container, comprising a series of eleven aluminium alloy rings stacked one above the other, and separated by an elastic medium, Figure 3. Several of these chambers have been constructed, and extensive dynamic analysis and testing has been carried out to determine their dynamic response characteristics, Butler (1999). The model container has internal dimensions of 627mm deep by 315mm wide by 796mm long. Each of the eleven aluminium alloy rings is 50mm high. The rings are not stiff enough along their long dimension to support the outward pressure from the soil inside under high g,

but they are supported by the massive reaction walls of the shaker unit itself. A rubber sheet separates the rings from the steel walls on either side. This concept has the added advantage of raising the center of gravity of the reaction mass in line with the center of gravity of the specimen, thus minimizing eccentric forces that may lead to rocking.

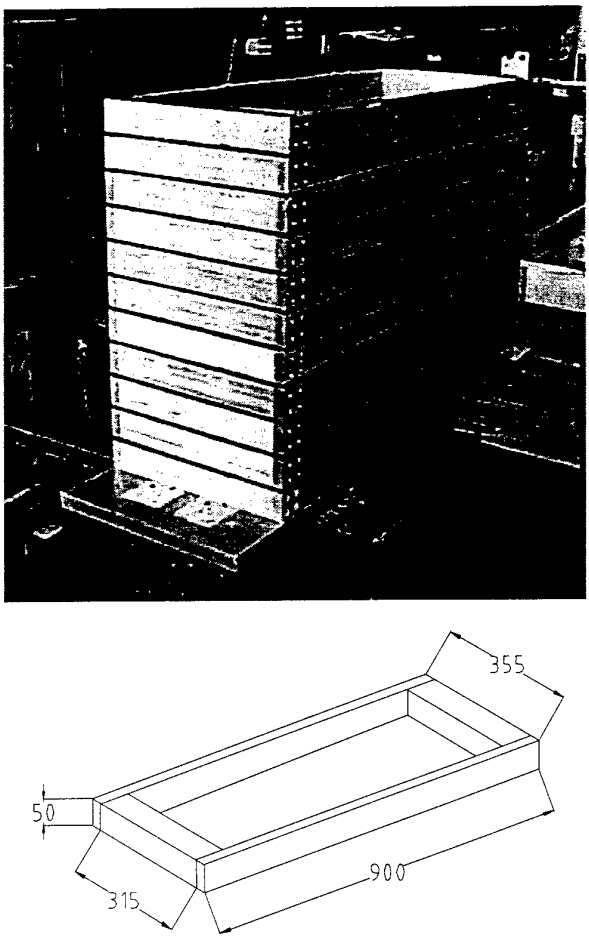

Figure 3. Typical Equivalent Shear Beam specimen container

Thin metal sheets, termed shear sheets, are positioned on the interior end walls of the chamber and fixed securely to its base. The shear sheets accommodate the complementary shear force generated by the horizontal shaking within the specimen and transmit that force to the base of the container, Figure 4. This improves the uniformity of the stress field at each elevation along the model, reducing the tendency for the chamber to 'rock'.

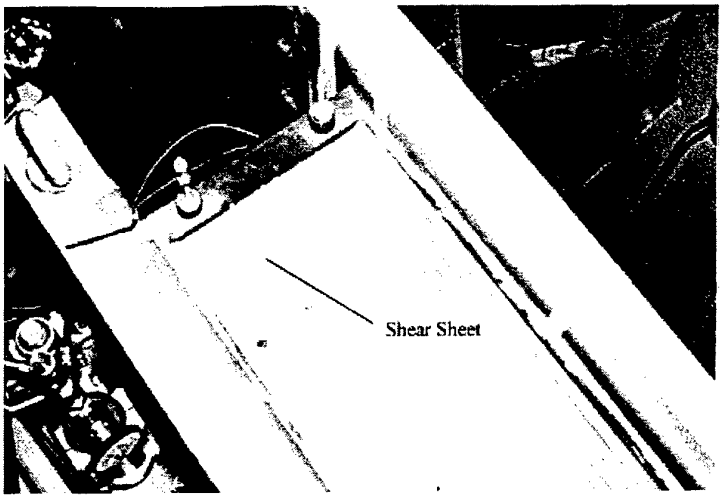

Figure 4. Shear sheets form the boundaries on the end walls of the ESB

The ESB concept is to create an equivalent shear beam with an average stiffness comparable to the stiffness of the soil specimen. Expressed rigorously, the concept is more accurately defined as achieving a dynamic response that does not significantly influence the behavior of the soil specimen inside. In certain classes of experiment, where the zone of interest is limited to the central region of the chamber, it may be expected that the stiffness of the soil (at least near the end walls) would not reduce significantly during shaking due to excess pore pressure rise. In this case the stiffness of the chamber may be designed accordingly, perhaps considering a shear modulus appropriate to the level of dynamic strain expected in the soil free-field at mid-depth. For other experiments involving the liquefaction of large volumes of soil inside the container, the stiffness changes (and hence dynamic response) will change dramatically throughout the base shaking. A stiff chamber may lead to undesirable effects, as noted by Peiris (1999) who observed that liquefaction in a loose saturated sand model did not occur near the stiff end walls of the chamber. A chamber with no stiffness simply adds mass to the soil specimen, again changing its dynamic response. This poses a particular challenge for the design of an ESB container.

The ERDC ESB used in these experiments was assembled using a urethane adhesive sealant (commonly used as a windshield sealant for cars) between the aluminum alloy rings. This material has good elastic properties (exhibiting only minimal hysteresis under cyclic loading) and bonded well to the metal and to itself. The ESB has a relatively low shear stiffness of 441 KN/m^2 (shear stiffness of the full stacked ring assembly) and mass of 229 kg, with a first mode at 16Hz, and second, third, and fourth modes at 46, 87, and 116Hz respectively (Butler 1999). A typical saturated specimen at 50g in the ERDC ESB will have a theoretical natural frequency of around 84Hz, based on an average small strain shear modulus of 96 MN/m^2.

3.3 Dynamic response of the model container and specimen

In his doctoral thesis, Butler (1999) completed a thorough theoretical and experimental analysis of the dynamic response of the coupled soil-container system. At high g the soil and container act as a coupled system, where the lower stiffness of the container reduces the natural frequency (slightly) of the combined system compared to the soil column alone. However, provided the driving frequency is low relative to the natural frequency of the coupled system, Butler (1999) demonstrates that the displacement response of the system is unaffected compared to the soil acting independently, an ideal situation.

For higher driving frequencies, Butler (1999) concludes that it would be necessary to reconsider the elastic stiffness of the ESB container, and to tune the container to ensure that even with the expected level of degradation in the soil specimen, the coupled system did not deviate significantly from the condition of the soil column alone. This may be possible by adding mass to the rings of an initially stiffer ESB to reduce its first mode to the desired level, Butler (1999).

The liquefaction of a level sand bed has previously been the subject of other research. Experiments were conducted at many centrifuge centers under the VELACS project, Arulanandan and Scott (1994). The objective of the ERDC study is to investigate the onset of liquefaction under much higher initial effective overburden stresses.

4.0 RESEARCH PROGRAM

Table 1 summarises the experiments conducted during 1998 and 1999. The models are grouped in series, where each series corresponds to a different target range of vertical effective overburden stress in the loose layer.

Model series	Models in series	Effective overburden stress in loose layer	Depth of prototype (approx)	Depth of specimen	Notes
2	a, b, c, d, e, f	1 tsf	15 m	300 mm	Nevada sand
3	a, b, c, d, e	2 tsf	26 m	525 mm	Nevada sand
4	a, b, c, d	3 – 5 tsf	26 – 40 m	525 mm	Nevada sand with lowered w.t. or surcharge
5	a, b, c, d	7 – 10 tsf	54 – 63 m	525 mm	Nevada sand with lead surcharge

Table 1. Summary of model tests

In all cases, the bottom 160mm of the specimen was around 50% Relative Density (RD) and the upper portion was around 75% RD. All models were shaken at 50g. Some models were overconsolidated by a factor of 2.5 prior to shaking (achieved by running the centrifuge up to 125g). A large series of experiments have been conducted with a range of overburden depths to provide repeatability and

redundancy in the instrumentation and data records. All the models were built using Nevada sand and tested at 50 g. The experiments are summarized in Table 2.

Model Code	Overall depth (mm)	Relative Density	σ_v' at mid-depth in loose layer (tsf)	OCR	Number of earth-quakes	Comments
2a	300	44% loose 83% dense	1	1	3	Saturated to ground surface.
2b	300	50% loose 75% dense	1	1	2	Saturated to ground surface.
2c	300	49% loose 74% dense	1	1	5	Saturated to ground surface.
2d	300	50% loose 75% dense	1	1	4	Saturated to ground surface.
2e	300	49% loose 73% dense	1	2.5	4	Saturated to ground surface.
2f	300	50% loose 75% dense	1	2.5	4	Saturated to ground surface.
3a	525	34% loose 73% dense	2	1	2	Saturated to ground surface.
3b	525	49% loose 77% dense	2	1	3	Saturated to ground surface.
3c	525	49% loose 79% dense	2	1	3	Saturated to ground surface.
3d	525	54% loose 80% dense	2	2.5	4	Saturated to ground surface.
4a	525	49% loose 80% dense	3	1	4	Saturated to top of loose layer only.
4b	525	56% loose 74% dense	3	2.5	4	Saturated to top of loose layer only.
4c	525	50% loose 75% dense	4.7	1	4	Saturated to ground surface. Lead surcharge.
4d	525	50% loose 68% dense	4.7	2.5	4	Saturated to ground surface. Lead surcharge.
5a	525	51% loose 72% dense	7.4	1	4	Saturated to ground surface. Lead surcharge.
5b	525	49% loose 76% dense	7.4	2.5	4	Saturated to ground surface. Lead surcharge.
5c	525	52% loose 75% dense	9.2	1	3	Saturated to ground surface. Lead surcharge.
5d	525	57% loose 80% dense	9.2	1	1	Saturated to ground surface. Lead surcharge.

Table 2. Detailed summary of experiments

The Nevada sand used in the models was characterized by standard laboratory tests to determine parameters such as dry density and gradation. Table 3 presents key material parameters for this sand.

Specific gravity	2.64
Maximum void ratio	0.757 (density 93.8 pcf)
Minimum void ratio	0.516 (density 108.7 pcf)
D_{50}	0.18 mm (approx)
D_{10}	0.11 mm (approx)

Table 3. Nevada Sand (parameters as measured)

The pore fluid comprised a mixture of glycerine and water, 80% by weight for experiments conducted at 50g. Measurements of the viscosity of glycerine-water mixes at a range of temperatures and proportions show that the viscosity is sensitive to both parameters.

The density of a glycerine-water mix was calculated from:

$$\rho_m = \rho_g(m_g + m_w)/(m_g + \rho_g m_w)$$

where ρ_m is the density of the mix, ρ_g is the density of glycerine, m_g is the mass of glycerine, and m_w is the mass of water. Table 4. summarizes the properties of the glycerine-water solution used as the pore fluid.

Density	1200 kg/m^3
Viscosity	50 cs
Specific Gravity	1.26
Composition	80% glycerine-water mix (by weight)

Table 4. Parameters for pore fluid (as measured)

The models were poured dry from a hopper and saturated under vacuum, or slowly under gravity. Instrumentation was placed in the model as it was being constructed.

The typical arrangement of the model specimens for the different test series is shown in Figure 5. Instrumentation was positioned through the depth of the models, and comprised pore pressure transducers and accelerometers. The location of the instrumentation for Model 5b is shown in Figure 6.

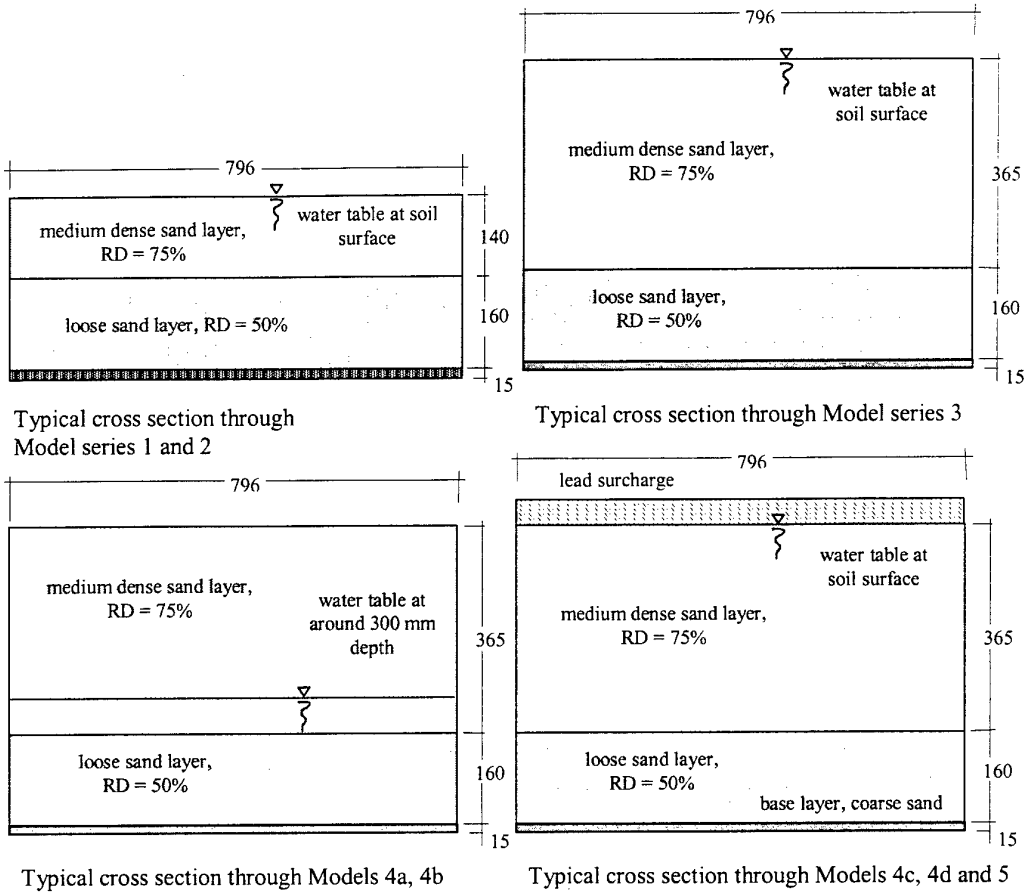

Figure 5. Cross sections through the different model configurations

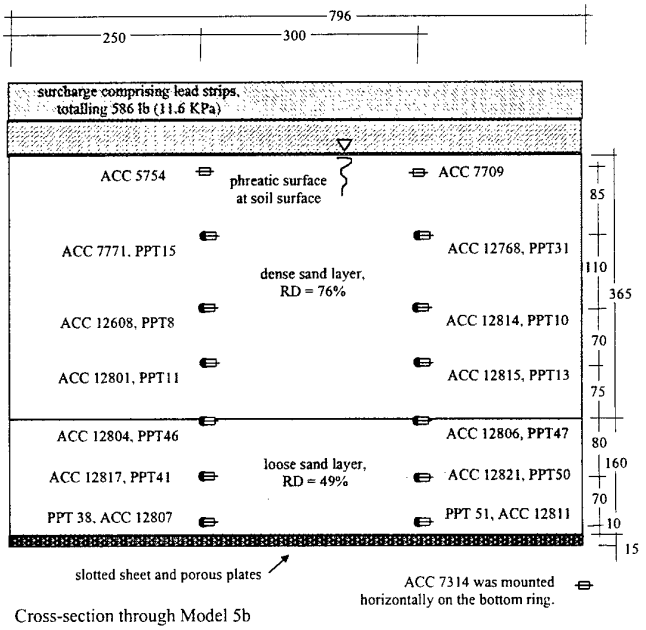

Figure 6. Instrumentation for Model 5b

5.0 AMPLIFICATION OF BASE INPUT MOTION

As the base input motion propagates through the height of the specimen, it may be amplified or attenuated depending on the dynamic properties of the soil column and the frequency content of the input motion. This is similar to conditions in the field, where elastic wave energy is modulated as it passes through different soil deposits. Examination of the time histories of acceleration at different depths in a deep soil column such as Model 5b, Figure 6, shows that in the absence of significant degradation caused by large strains or excess pore pressures, the amplification factor is around 1, Figure 7. A similar response was also found for shallow specimens. In specimens where large excess pore pressures started to develop through the soil column, however, the characteristics of the motion propagating upwards tended to change dramatically. In the extreme, the lateral accelerations of the surface becomes isolated from the base input, as may be seen in Figure 8 which shows the acceleration at different depths in Model 2f.

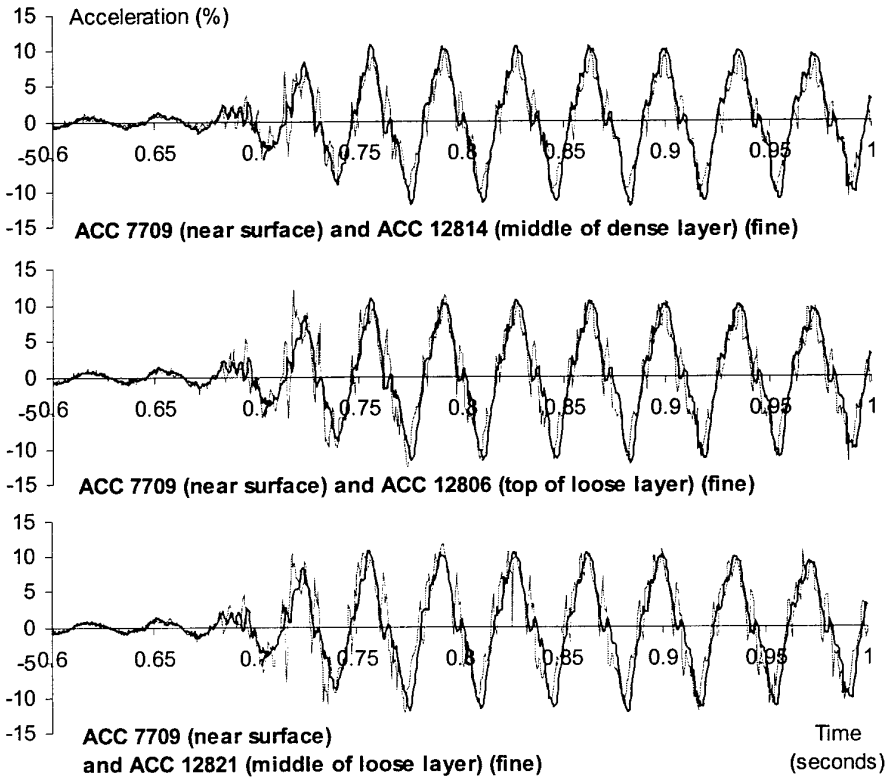

Figure 7. Comparison of the measured surface acceleration with the acceleration at different depths, Model 5b

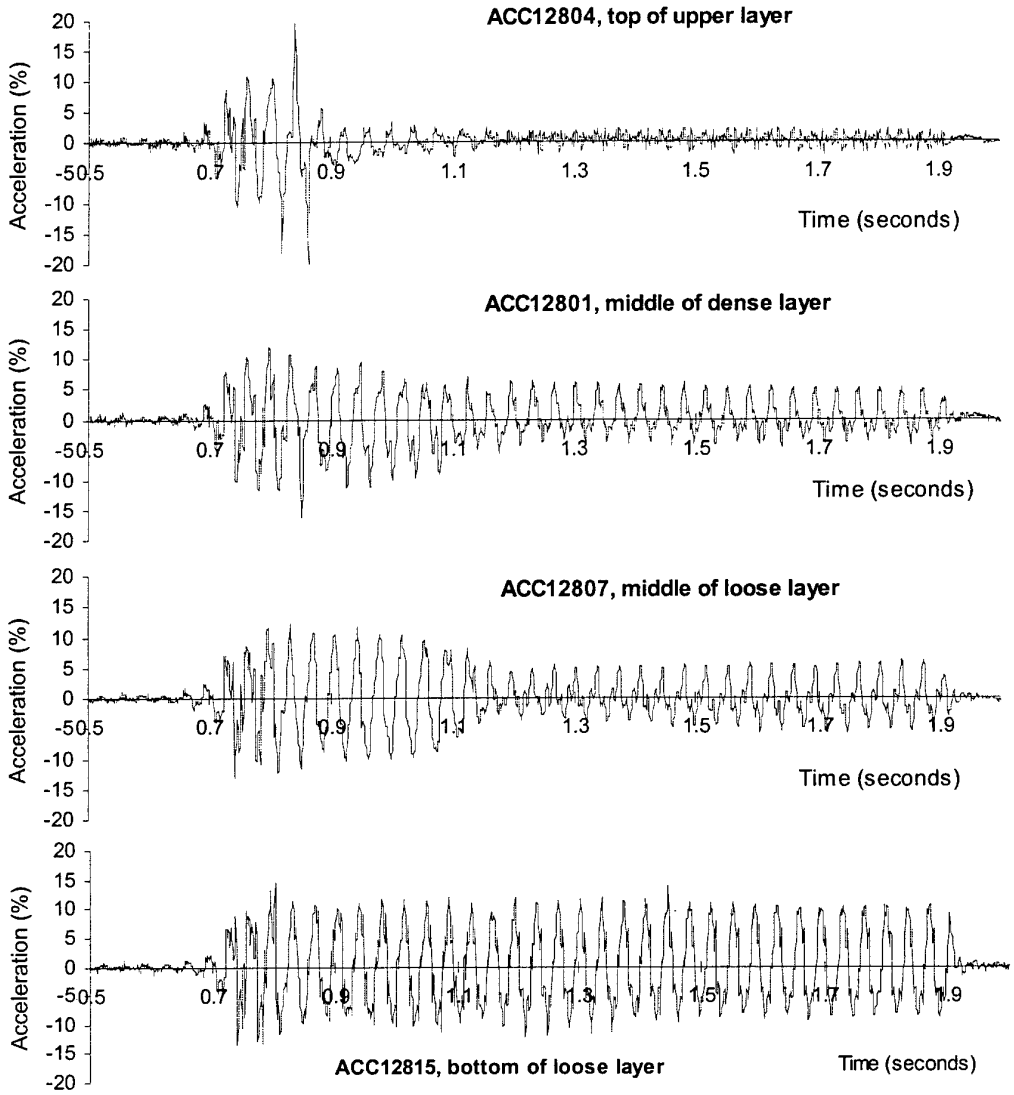

Figure 8. Comparison of measured accelerations at different depths, Model 2f

6.0 DEVELOPMENT OF EXCESS PORE PRESSURES AND LIQUEFACTION AT SHALLOW DEPTHS

The target initial effective vertical stress in Model 2f was 1 tsf (100 KPa) at mid-depth in the loose layer (Table 2). The specimen was overconsolidated by accelerating the centrifuge to 125g prior to subjecting it to shaking motion at 50g. Figure 9 shows how the excess pore pressures at different depths developed with time. It is clear that within a few cycles of shaking, the loose sand layer has fully liquefied.

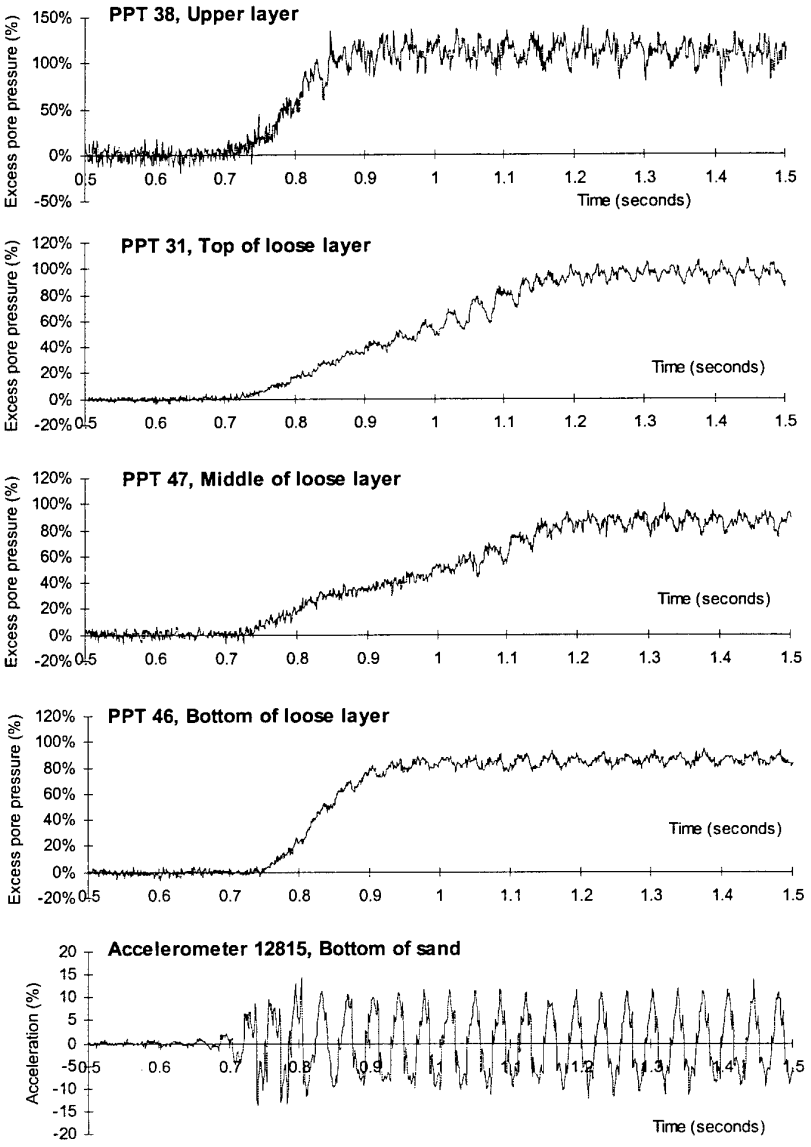

Figure 9. Development of excess pore pressure in a shallow bed, Model 2f

Comparison between the acceleration time histories in Figure 8 and the excess pore pressures in Figure 9 for the loose and dense layers shows the correlation between transmitted motion and level of excess pore pressure. The upper section (near surface) of the dense layer liquefies within 0.2 seconds (0.2 x 50 = 10 seconds field equivalent). The percentage of excess pore pressure is calculated by dividing the measured fluid pressure by the calculated initial overburden stress. The actual overburden stress may vary over time due to small movements of the transducer in the liquefied ground; this has a larger effect on the accuracy of measurement at shallower locations, such as PPT 38.

It is interesting to note that despite the difference in relative density between the dense and loose layers, the soil column behaves more like a single unit than as two layers. This is because each increment of excess pore pressure at depth immediately causes a fluid pressure, which affects the whole column through the volumetric compressibility of the pore fluid. This is considerably lower than the shear compressibility of the soil skeleton, which is determining the speed of transmission of the elastic shear wave upwards.

This finding has important consequences for the assessment of the response of a soil column comprising dense over loose layers. The dense layer cannot be assumed to act independently of the underlying loose layer, at least where no impermeable layer clearly separates the two deposits. The effect of including an impermeable layer on the response of the column is recommended as a priority for future research.

(A similar finding to this was observed in centrifuge model experiments during the 1980s, where loose 'pockets' were present in relatively shallow layers of saturated sand supporting a clay dyke and subject to strong base shaking, at Cambridge University for Intevep SA, Venezuela, Steedman and Habibian (1987). Here also, the incompressible nature of the pore fluid led to instantaneous interaction between the dense and loose zones, with the overall response dominated by the geometry of the dyke on its foundation.)

7.0 GENERATION OF EXCESS PORE PRESSURES AT HIGH CONFINING STRESS

At high initial effective confining stress pore pressures are also observed to rise strongly during the initial cycles of shaking. After some time, this steady rise is arrested, and then excess pore pressure is capped at a value less than the full 100% of the initial vertical effective stress seen in shallow soil columns. Figure 10 shows a set of data from Model 4d, a deep soil specimen with an initial effective vertical stress of around 500 KPa (4.7 tsf) at mid-depth in the loose layer.

A similar picture was found at even higher initial vertical effective stress. Figure 11 shows the development of excess pore pressure under a vertical effective stress in the middle of the loose layer of 1037 KPa (9.7 tsf). In this figure, the actual fluid pressure has been plotted in KPa, to be compared with the initial vertical effective stress. The time history of base shaking is shown below the pore pressure record in two forms. The first trace shows the measured record, which includes a degree of high frequency noise. In the second, lower trace, this signal has been processed with a Butterworth band pass filter, 250 and 10 Hz, to extract the main shaking frequency. From this record, it is clear that the amplitude of the shaking motion is almost constant throughout the record, and particularly that the amplitude remains at or near its peak level throughout the second half of the shaking episode, when the excess pore pressure has been capped (after about 0.8 seconds of shaking, or 40 seconds field equivalent). In this case, the excess pore pressure is capped at around 50% of the value required to reach 'initial liquefaction'.

The amplitude of cyclic shaking was easily sufficient to generate excess pore pressures at a strong rate during the first half of the event, and this can be seen in the top trace of Figure 11. Indeed, after around 0.4 seconds of shaking the rate of excess pore pressure build-up increases, and this may be related to a moderate increase in the amplitude of base shaking at the same time. Between around 0.4 seconds and 0.7 seconds of shaking the rate of increase of excess pore pressure is around 350/0.3 ~ 1000 KPa/second (or 20 KPa/second field equivalent). The driving frequency of input motion is around 50 Hz (1 Hz field equivalent). During the same period, the amplitude of shaking is around +/- 15% g, which corresponds to a cyclic displacement of +/- 0.76 mm (38 mm field equivalent) at that depth.

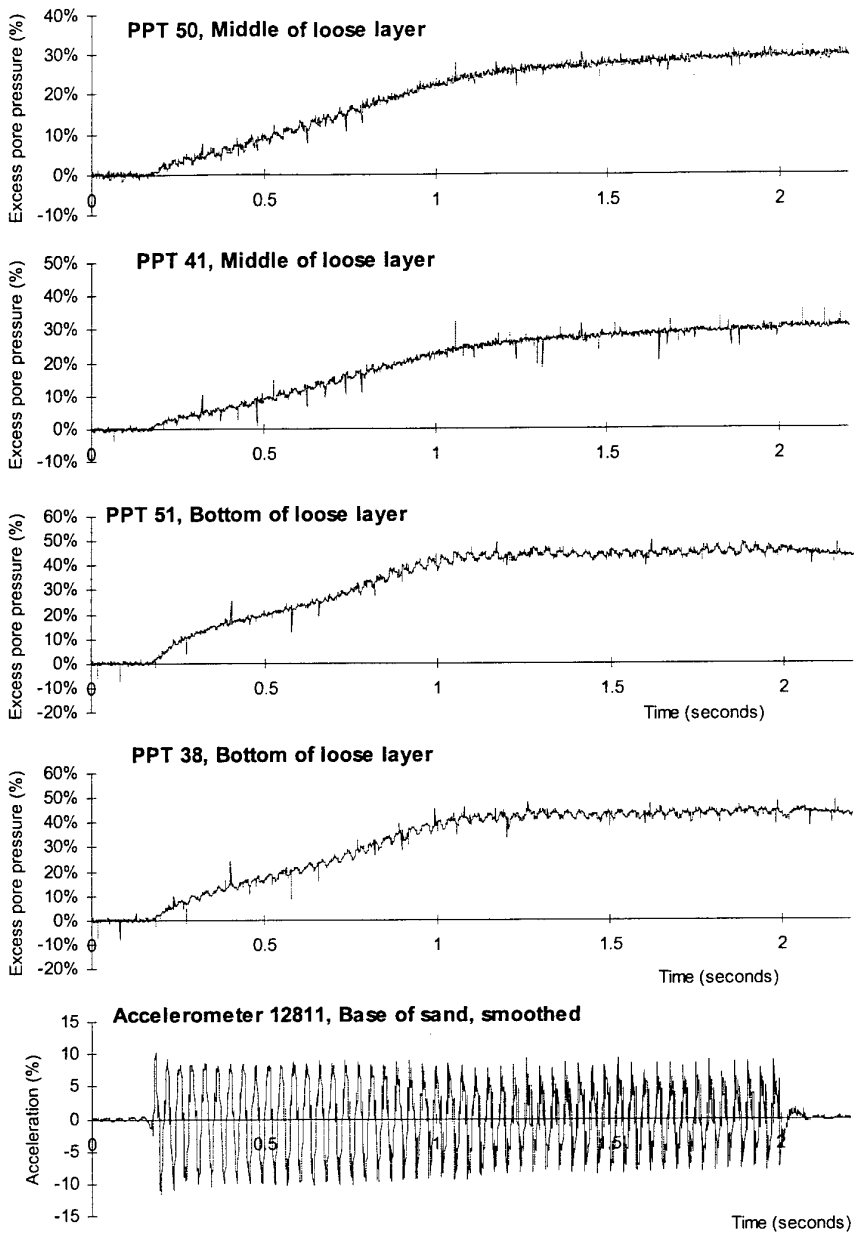

Figure 10. Development of excess pore pressure at over 500 KPa, Model 4d

This pattern of behavior was found in all specimens at initial vertical effective confining stresses of around 250 KPa or greater. Although not a rigorous comparison, as there are a number of variables (including amplitude) between the different experiments, Figure 12 shows the normalised results from a range of initial conditions. There is a general trend with increasing initial vertical effective stress, towards the capping of excess pore pressure at a level lower than the expected 100%.

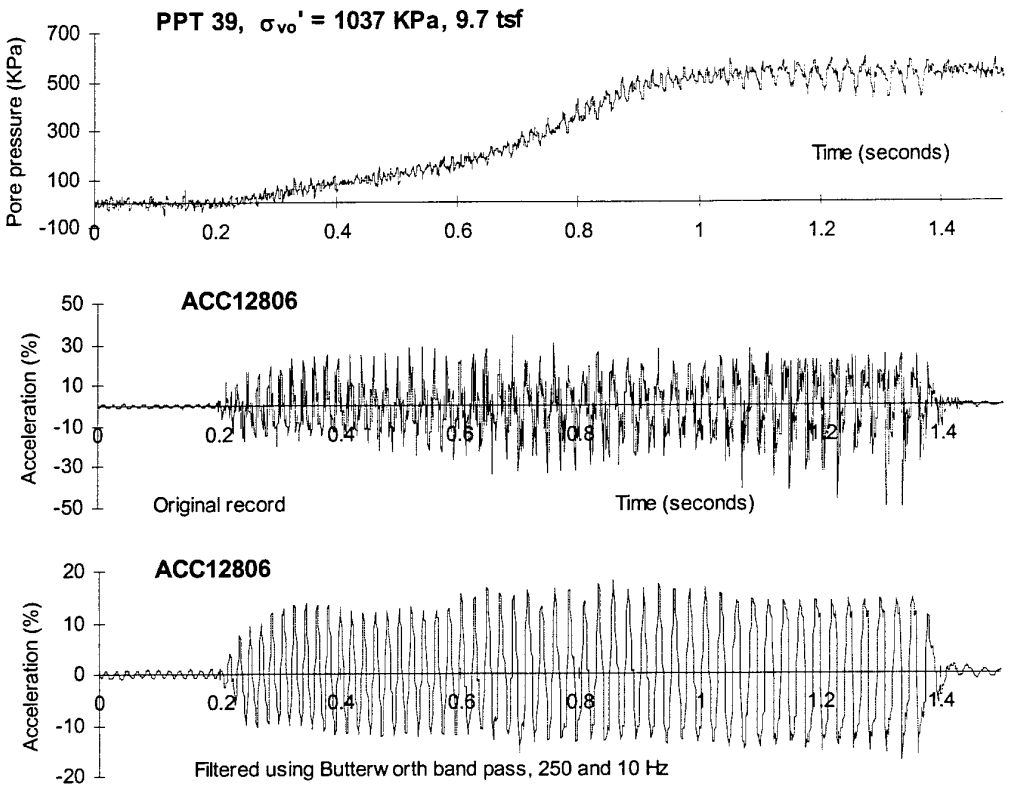

Figure 11. Development of excess pore pressure at initial vertical effective stresses of up to 1000 KPa (10 tsf), Model 5d

All of the records of excess pore pressure from all the model specimens were re-examined to determine the residual pore pressure at the level of capping. Although the amplitudes of shaking and the densities of the sand varied (the data-set includes both 'dense' and 'loose' sand layers as described above) a clear correlation was found between the maximum level of excess pore pressure and the initial vertical effective stress, as shown in Figure 13. This figure includes 125 data points from first and succeeding earthquakes, normally and overconsolidated specimens, and dense and loose layers.

Figure 14 shows the data from first earthquakes only, broken out by normally consolidated and overconsolidated (including dense and loose results). Again, there is a strong correlation between the maximum level of excess pore pressure generated during the shaking and the initial vertical effective stress. In this case, the overconsolidated data is seen to lie to the left of the normally consolidated data, indicating that the level of excess pore pressure may reduce for increased overconsolidation. This is consistent with experience.

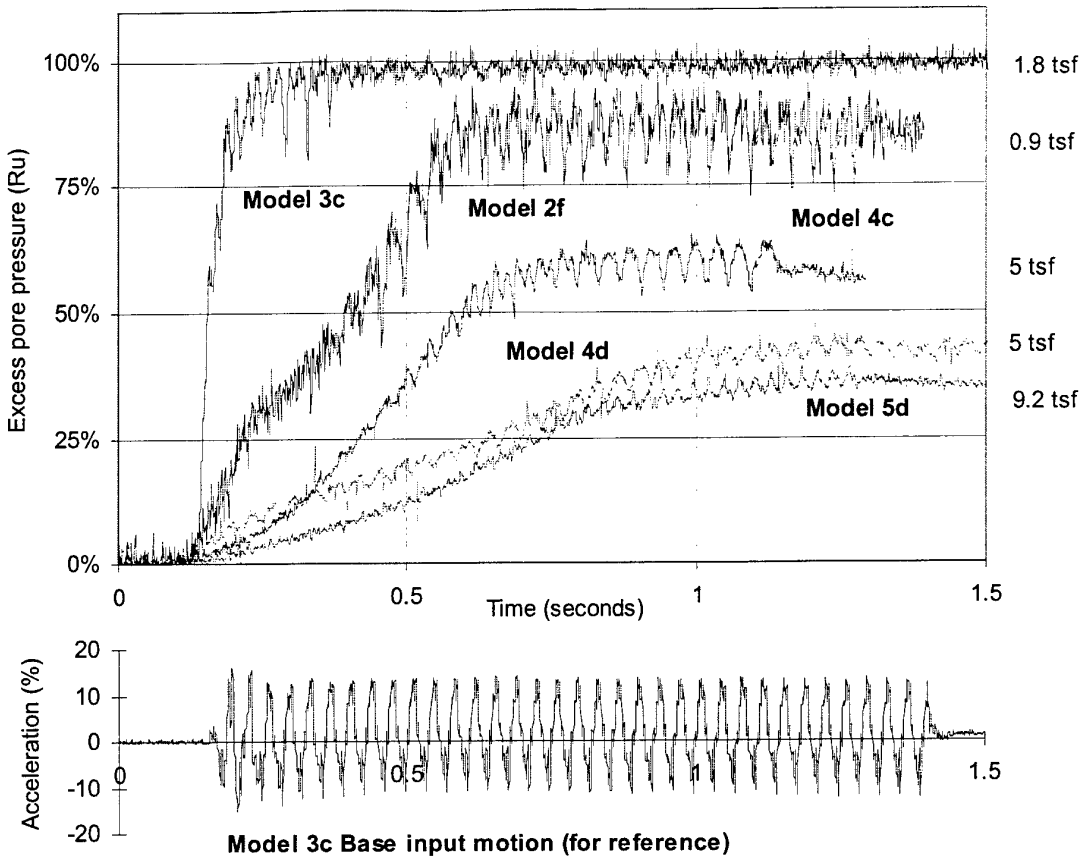

Figure 12. Comparison between excess pore pressure development at different initial vertical effective stresses

On the right hand side of Figures 13 and 14, an approximate depth scale has been given for guidance, expressed in feet. Clearly the calculation of equivalent field depth depends on many assumptions, but it is worth noting that the data appear to show that whilst liquefaction may readily occur within the upper 40 feet or so of a saturated sand deposit, it becomes increasingly unlikely at greater depths. This is consistent with field observation.

Further research work has been proposed with a view to full verification of these findings and the preparation of design guidance. Further experiments will address the effects of amplitude of shaking, sloping ground and density. To achieve the primary objective of increased amplitude of shaking, the MkI earthquake shaker was replaced during the summer of 2000 with the MkII.

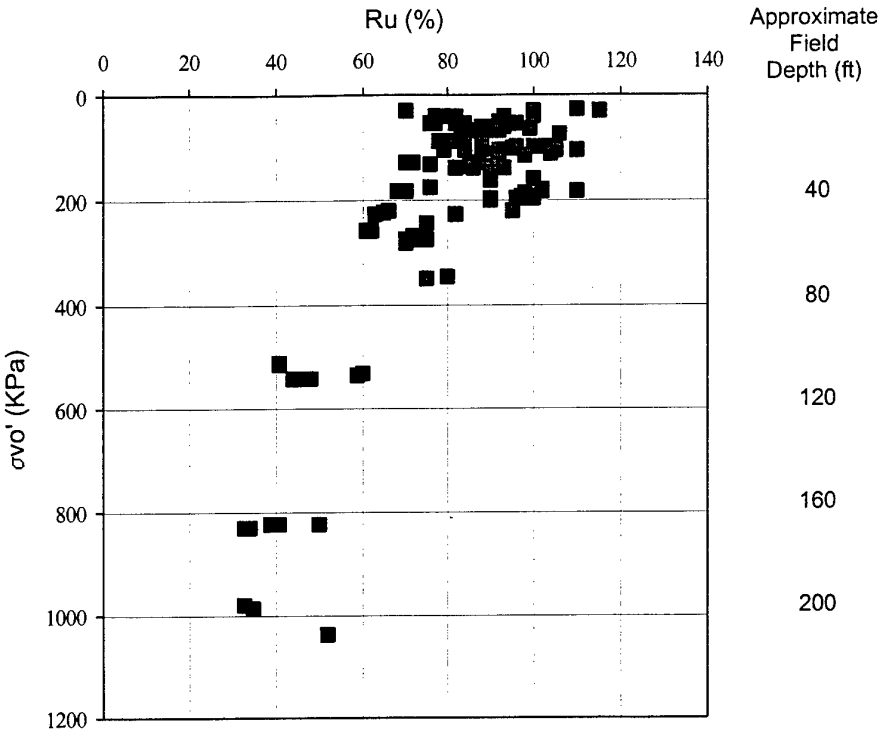

Figure 13. Comparison between maximum residual excess pore pressure and initial vertical effective stress, all data

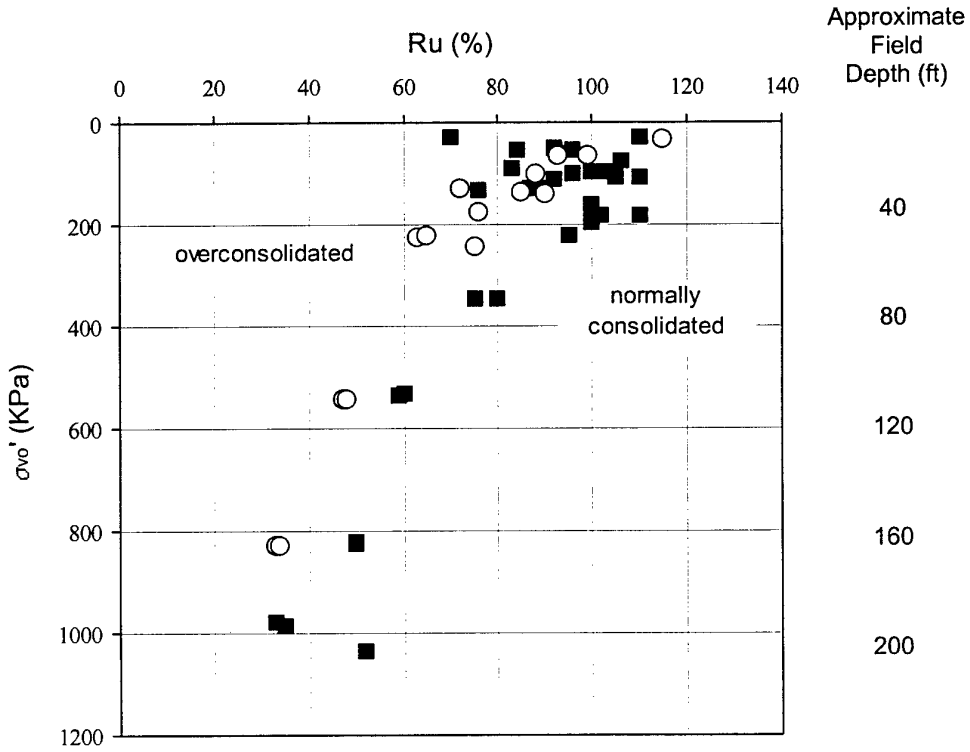

Figure 14. Comparison between overconsolidated and normally consolidated data, all data

8.0 CONSEQUENCES FOR A HYPOTHETICAL LARGE EARTH DAM

To illustrate the potentially highly significant consequences of capped pore pressures decreasing with depth, a hypothetical earth dam of the form outlined in Figure 15 is assessed. The estimated deformation response is calculated for earthquake induced potential pore pressures based on standard approaches, Seed and Harder (1990), Youd and Idriss (1997), and on limiting pore pressure generation. Deformations are estimated following the procedures of Ledbetter and Finn (1993), Finn et. al. (1995), and Ledbetter et. al. (1994b), with the use of the non-linear dynamic effective stress analysis program TARA, Finn el. al. (1986), and Finn and Yogendrakumar (1989).

The dam is located across stream channel deposits with assumed profile, Figure 15, as: (a) foundation older stiffer alluvium below elevations 151 m (u/s) - 163 m (d/s), (b) younger less stiff alluvium above the older alluvium, and (c) roller compacted zoned earth dam founded on the young alluvium. Crest level and Pool level are 211m and 199m respectively. Standard Penetration $(N_1)_{60}$ values range from 5 to 15 and shear-wave-velocity (V_s) from 180-450 m/s in the young alluvium freefield upstream and downstream. Beneath the dam, the young alluvium downstream $(N_1)_{60}$ values range from 30 – 40 and V_s from 425-700 m/s and upstream $(N_1)_{60}$ values range from 6-20 with V_s from 150-350 m/s. Ground motions are assumed to be from a magnitude 7.75 earthquake occurring at a distance from the dam about 50 miles with a peak acceleration of 0.22g at the dam.

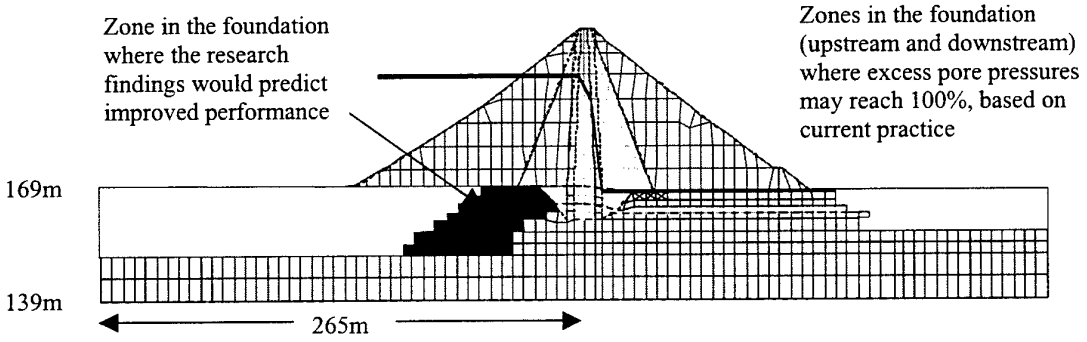

Figure 15. Comparison of affected zones in the foundation

8.1 Maximum potential residual excess pore pressure

Seed's simplified procedures (Seed and Harder, 1990) were coupled with non-linear dynamic effective stress finite element analysis to yield "field observation and laboratory based" estimates for earthquake induced pore pressures. These pore pressures are considered the "maximum potential residual excess pore pressures" that that could be generated by the design earthquake, based on historic field earthquake response. Unless the soils have low permeability and/or are bounded by low permeability layers that prevent the dissipation of excess porewater pressures, earthquake-generated porewater pressures should be less than the maximum potential.

For this example dam, Figure 15 shows the maximum potential residual excess porewater pressures (shaded zones) that can be generated by the design earthquake. The young alluvium can generate pore pressures (a) downstream of the downstream toe but nothing of significance beneath the downstream shell and (b) upstream of the upstream toe and beneath the upstream shell. The lighter shaded upstream zone extends completely beneath the darker shaded zone. Pore pressures in these lighter shaded zones are between 80 – 100 % of the initial vertical effective stress with the majority between 90 and 100 %.

The research findings expressed in this paper are for level ground conditions. Continuing research is recommended to address the effects of residual shear stresses such as induced by the geometry of a dam. Until the geometry effects are known, this example applies the pore pressures trend shown in Figure 14 for the normally consolidated case as the cap or limitation. In this example, the zone of soil that will be effected and have reduced pore pressure potential is the darker shaded zone beneath the upstream shell; quite naturally, this is a high confining stress zone and where K_σ leads to a strength reduction due to the high confinement. This zone is exactly where strength increase or less strength degradation is of prime importance to the dam behavior under earthquake loading. The pore pressure potential in the darker shaded zone is reduced from 80 – 100 % to 50 –75% of the vertical effective stress.

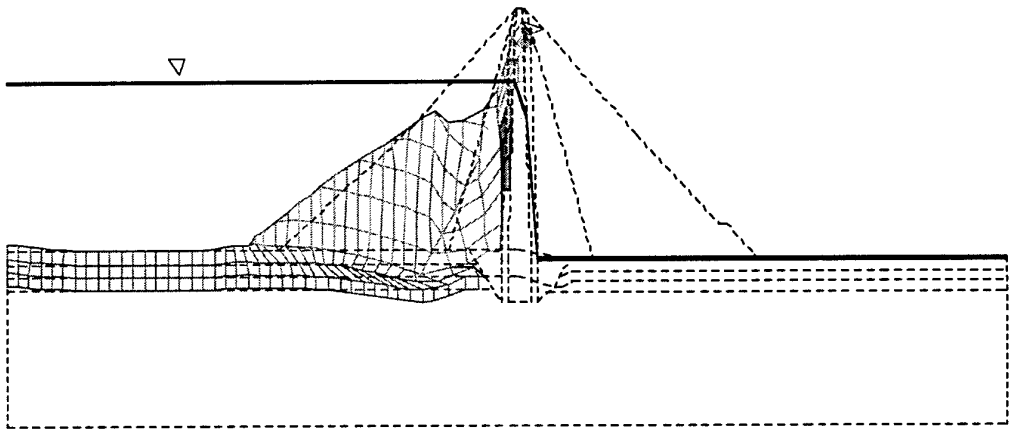

Figure 16. Deformations calculated using current analyses

8.2 Deformation response of the dam

Figures 16 and 17 illustrate the effects or differences in earthquake induced deformations and strains caused by the applied pore pressure limits. For the deformation stage shown in the figures, the only elements that appear shaded are those significantly straining and participating. Figure 16 shows the deformations at effective strength reduction to 72 % of the initial caused by pore pressure increase. The dam will continue to deform as pore pressure builds to the maximum potentials and residual strength is reached beneath the dam in the foundation, which is around 90 % reduction of initial strength. Unless remediated,

severe earthquake damage to the dam is possible accompanied by overtopping and piping through the core resulting in complete failure.

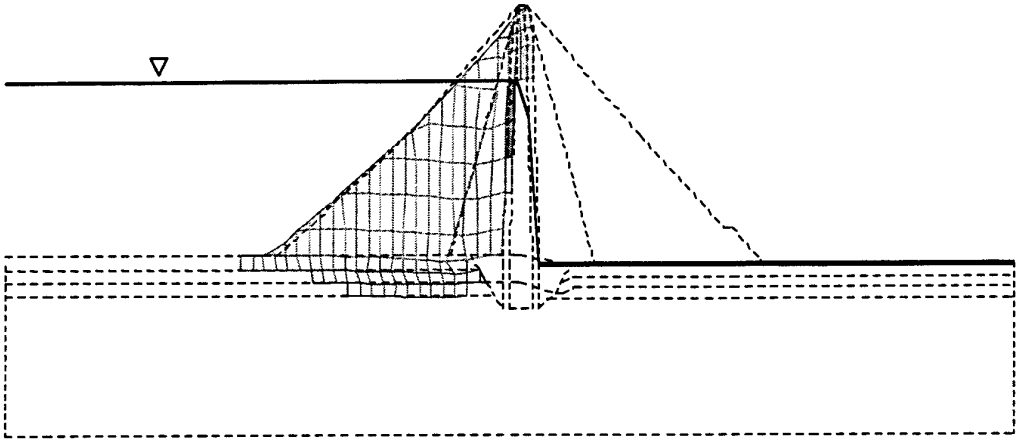

Figure 17. Deformations predicted using pore pressure limits and improved soil strength

Figure 17 illustrates the benefits achieved by applying the limiting pore pressure with depth trend. The deformation stage in Figure 17 is the same as that in Figure 16. As shown strains, deformations and the active elements are significantly reduced. The dam continues to deform as pore pressures increase to their maximum potentials and residual strengths; however, the final stages of deformation are considerably less than those under the conditions in Figure 16.

Immediately obvious from comparison of Figures 16 and 17 is that more strength is available to resist deformation movements and to buttress and assist remedial treatments. The availability of more strength translates to smaller and less remediation and lower costs. The stage of progressive strength reduction illustrated in both Figures 16 and 17 was chosen to best exemplify the impact of limiting pore pressure criteria on dams with liquefiable soils in high initial effective confining stress fields.

The implication of the present study is that although soil at depth may soften and degrade under earthquake induced excess pore pressure behavior, the reduction in strength is limited and liquefaction under high confining stresses may not be the hazard that it is presently assumed to be.

9.0 CONCLUSIONS

1. A large data-set of the behavior of loose saturated sands under high initial effective confining stresses and subject to earthquake-like shaking has been collected during an extensive experimental program on the ERDC Centrifuge, Vicksburg MS.

2. This data has shown that, at moderate amplitudes of excitation, the maximum level of excess pore pressure development is capped at high initial effective confining stress and does not reach a level sufficient to cause 'initial liquefaction' (defined as 100% of the initial vertical effective stress).

3. These findings are currently being verified and will then be used to develop appropriate design guidance.

4. High pore pressures and the potential for liquefaction beneath dams may not be the hazard that it is currently perceived to be.

5. The implication for the assessment of liquefaction hazard and requirements for remediation works under large earth dams is potentially very significant.

10.0 REFERENCES

Arulanandan, A. and Scott, R.F. (1994) editors, Proc. Int. Conf. on Verification of Numerical Procedures for the Analysis of Soil Liquefaction Problems, at U.C. Davis; Volumes 1 & 2; Balkema.

Butler, G.D. (1999). A dynamic analysis of the stored energy angular momentum actuator used with the equivalent shear beam container, PhD thesis, Cambridge University (in preparation).

Finn, W.D.L. and Yogendrakumar, M., Yoshida, N. and Yoshida, H., (1986), "TARA-3: A Program to Compute the Response of 2-D Embankments and Soil-Structure Interaction Systems to Seismic Loadings", Department of Civil Engineering University of British Columbia, Canada.

Finn, W.D.L., Ledbetter, R.H., and Marcuson, W.F. III (1995). "Seismic Deformations in Embankments and Slopes", Symposium on Developments in Geotechnical Engineering - From Harvard to New Delhi, 1936-1994, Bangkok, Thailand, A.A. Balkema, Rotterdam.

Finn, W.D.L. and Yogendrakumar, M., (1989) "TARA-3FL; Program for Analysis of Liquefaction Induced Flow Deformations", Department of Civil Engineering, University of British Columbia, Vancouver, Canada.

Ledbetter, R.H. (ed) (1991) Large centrifuge: a critical Army capability for the future, Misc. Paper GL-91-12, Dept. of the Army, Waterways Experiment Station, Vicksburg, MS, May.

Ledbetter, R.H., and Finn, W.D.L. (1993). "Development and Evaluation of Remediation Strategies by Deformation Analysis", ASCE Specialty Conference on Geotechnical Practice In Dam Rehabilitation, Raleigh, North Carolina, April, pp 386 - 401.

Ledbetter, R.H., Steedman, R.S., Schofield, A.N., Corte J.F., Perdriat J., Nicholas-Font J. and Voss H.M. (1994a) US Army's engineering centrifuge: Design, Proc. Centrifuge 94, pp63-68, Singapore, 31 Aug – 2 Sept, Balkema.

Ledbetter, R.H., Finn, W.D.L., Hynes, M.E., Nickell, J.S., Allen, M.G., and Stevens, M.G. (1994b). "Seismic Safety Improvement of Mormon Island Auxiliary Dam", 18th International Congress on Large Dams, Durban, South Africa.

Ledbetter, R.H., Steedman, R.S. and Butler, G.D. (1999) Investigations on the behavior of liquefying soils, Proc Int Workshop on Physics and Mechancs of Soil Liquefaction, Baltimore MD, Lade P.V. and Yamamuro J.A. (eds), 10-11 Sept 1998, Balkema, pp 295-306.

Peiris, L.M.N. (1999) Seismic modelling of rockfill embankments on deep loose saturated sand deposits, PhD Thesis, Cambridge University.

Seed H.B. (1983) Earthquake-Resistant Design of Earth Dams, Proceedings of Symposium on Seismic Design of Embankments and Caverns, May, ASCE pp 41-64.

Seed R.B. and Harder L.F. (1990) SPT-Based analysis of cyclic pore pressure generation and undrained residual strength, Proc. H Bolton Seed Memorial Symposium, Vol. 2, pp 351 - 376, BiTech Publishers Ltd, Vancouver.

Steedman R S and Habibian A (1987). Modelling the failure of coastal dykes during earthquakes. 9th European Conf. Soil Mech. Found. Eng. Vol 2, pp 633-636, Dublin, 31 Aug - 3 Sept.

Youd, L. and Idriss, I., Eds (1997) Workshop on Evaluation of Liquefaction Resistance of Soils, Proceedings, Salt Lake City, Technical Report NCEER-97-0022, sponsored by FHWA, NSF and WES, published by NCEER.